NORSAR

NORSAR Scientific Report No. 1-2005

Semiannual Technical Summary

1 July - 31 December 2004

Frode Ringdal (ed.)

Kjeller, January 2005

6 Summary of Technical Reports / Papers Published

6.1 The detection of rockbursts at the Barentsburg coal mine, Spitsbergen, using waveform correlation on SPITS array data

6.1.1 Introduction

In several previous Semiannual Technical Summaries, we have studied the detection and location of rockbursts at the Barentsburg coal mine on Spitsbergen. This work has been done in cooperation with the Kola Regional Seismological Centre (KRSC), which operates two seismic stations in the immediate neighborhood of the mine.

In this paper, we apply a waveform correlation procedure to Spitsbergen array data in order to obtain improved detection of such rockbursts. We use available data from the near-mine stations to verify the results, and we compare the results obtained by correlation processing to those obtained through conventional array processing methods.

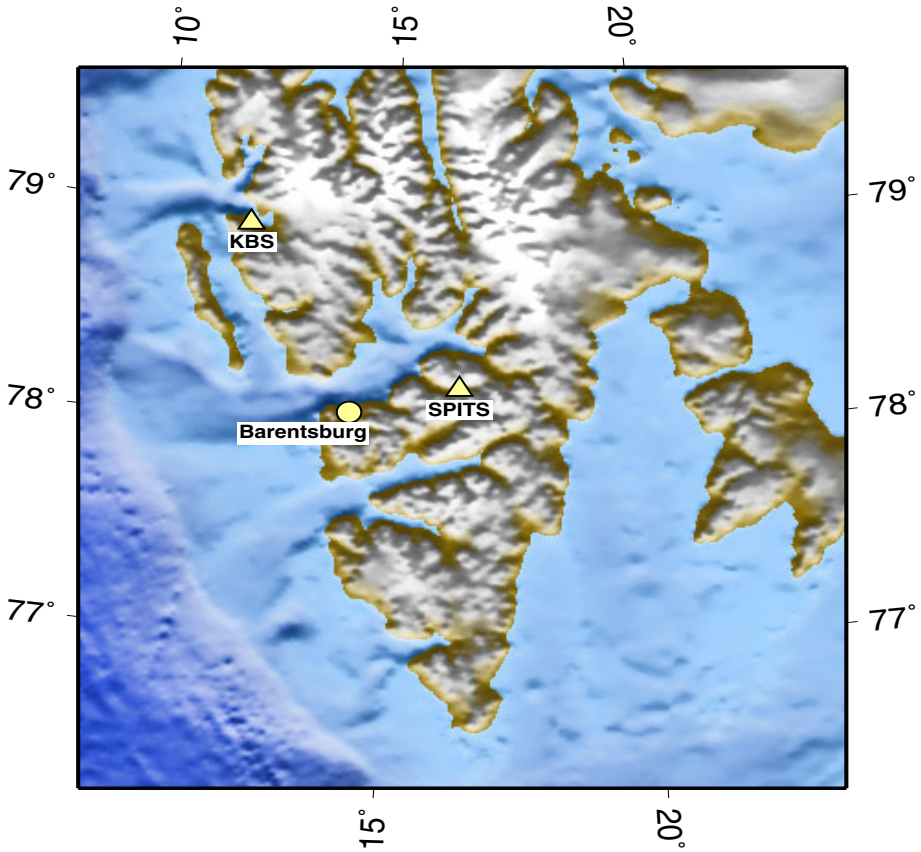

Fig. 6.1.1. Locations of the Barentsburg coal mine, the SPITS seismic array, and the KBS (Kings Bay, Ny Ålesund) 3-component seismic station on the Island of Spitsbergen.

On July 26, 2004, a rockburst at the Barentsburg mine led to the death of a mine worker; this was the third fatal mining accident at this site within four years. The mine is situated approximately 51 km to the west of the Spitsbergen array (see Figure 6.1.1) which recorded the seis-

mic signals from both this event and several previous rockbursts at the mine (see Kværna et al., 2003, Kremenetskaya et al., 2001).

Using data from both SPITS and the KBS 3-component station (at a distance of approximately 120 km), a magnitude estimate of 1.76 was obtained for the event together with origin time 2004-208:06.42.19.44 and coordinates 77.9375°N, 14.0703°E. The SPITS data from this event is displayed in Figure 6.1.2. In Figure 6.1.3, the waveforms from the July 26, 2004, are compared with those from three previous events within the coal mine. The waveforms from the different events display a high degree of semblance in the 1.2 - 2.5 Hz frequency band and far less similarity in the 2.0 - 4.0 Hz band.

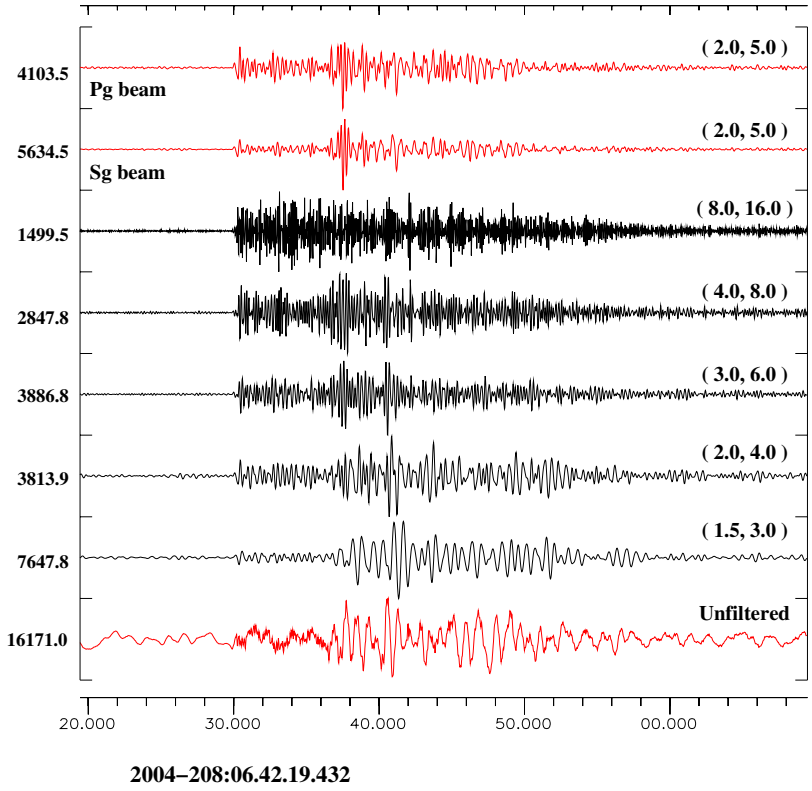

Fig. 6.1.2. Waveforms recorded at the Spitsbergen array resulting from the 26 July 2004 accident at the Barentsburg mine. All traces displayed are the SPA0_sz channel except for the top two traces which are the beams from all sz channels with (vel., azi.) = (5.8, 244) for Pg and (vel., azi.) = (3.4, 244) for Sg. The numbers to the left indicate the maximum amplitude and the frequency band is indicated to the right.

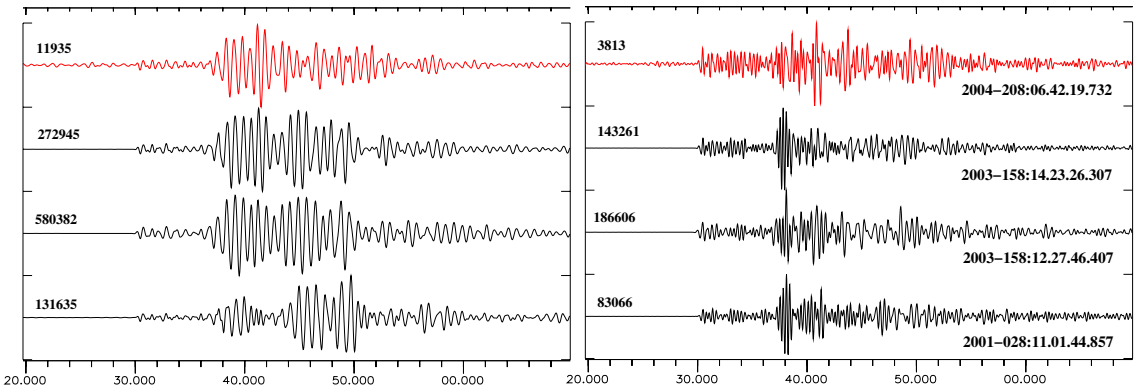

Fig. 6.1.3. SPA0_sz recordings of the July 26, 2004, event (red traces) together with recordings of three previous events in the Barentsburg mine. All traces are aligned according to the best correlation with a 5.0 second long window beginning at a time 2004-208:06.42.30; traces to the left are filtered between 1.2 and 2.5 Hz and traces to the right are filtered between 2.0 and 4.0 Hz.

The goal of the current work is to identify other events which may have occurred within close proximity of the site of the July 26 2004 rockburst and, subsequently, to evaluate the level of seismicity in the region prior to this collapse and examine how this seismicity varied with time. We wish to limit the set of events found to a very small geographical footprint and therefore use an array-based waveform correlation method similar to that described by Gibbons and Ringdal (2004). Whereas location estimates using traditional regional array techniques (see, for example, Ringdal et al. 2003) are likely to be associated with error ellipses of the order of several kilometers (even given the short distance of only 51 km between source and receiver), two events whose waveforms display a sufficiently high correlation are necessarily constrained to have taken place with a region limited by a small multiple of the wavelength at a dominant frequency (Geller and Mueller, 1980). It is also well known that many events too weak to be located adequately by traditional methods can be detected using a matched signal detector.

6.1.2 Event Detection Using Multi-Channel Waveform Cross-Correlation

For the preliminary investigation, a master waveform (a template), filtered between 3.0 and 6.0 Hz, was extracted with a starting time 2004-208:06.42.29.695 and length 20.0 seconds for each channel in the Spitsbergen array. The same time interval was chosen for all of the channels in the array for the sake of simplicity; the aperture of the array is sufficiently small that energy corresponding to a given phase arrives at all sites within less than a second. The fact that a phase arrives later at some stations than others is not an issue; a second event taking place at the same site will result in identically delayed arrivals. It is clear from Figures 6.1.2 and 6.1.3 that a 20.0 second long window includes most of the wavetrain including approximately 14 seconds following the Sg secondary phase arrival. The waveforms were resampled to 40 Hz in order to perform the cross-correlation. The choice of the 3.0 - 6.0 Hz frequency band, under the quarter-wavelength argumentation of Geller and Mueller (1980), constrains the locations of two well-correlated events to be within approximately 150m of each other (based upon a velocity of 3.5 kms^{-1} at a frequency of 6 Hz). However, the “correlation distance” of two different events is likely to vary greatly with local structure and heterogeneity (see, for example, Nakahara 2004); measurements at local distances would be required to verify precise location estimates.

The detection procedure, described by Gibbons and Ringdal (2004), is illustrated in Figure 6.1.4. A continuous, fully-normalised, correlation coefficient is calculated between the data following a given time point and the extracted template waveform for each channel in the array. A zero time-delay beam is then formed from all the correlation traces. A detection is made when the scaled correlation trace (the top channel in Figure 6.1.4) exceeds a preset value, analogous to an SNR threshold in a conventional STA/LTA detection. Specifying a threshold on the scaled trace was found by experience to be considerably easier than specifying an absolute value of the correlation coefficient as a threshold. Correlation coefficients vary greatly depending upon the nature of the signal, in particular the time-bandwidth product of the template waveform, and also on the number of channels used in the array or network. To be able to specify a detection threshold for such a trace requires considerable calibration for each calculation attempted. The scaled correlation beams were examined for a wide range of scenarios and were found to vary typically between -3.5 and +3.5 in the absence of any obvious detections and to very rarely exceed 4.5 unless accompanied by an abnormally high correlation coefficient. A value of 6.0 was found to be quite a robust detection threshold for the majority of scenarios without systematic calibration.

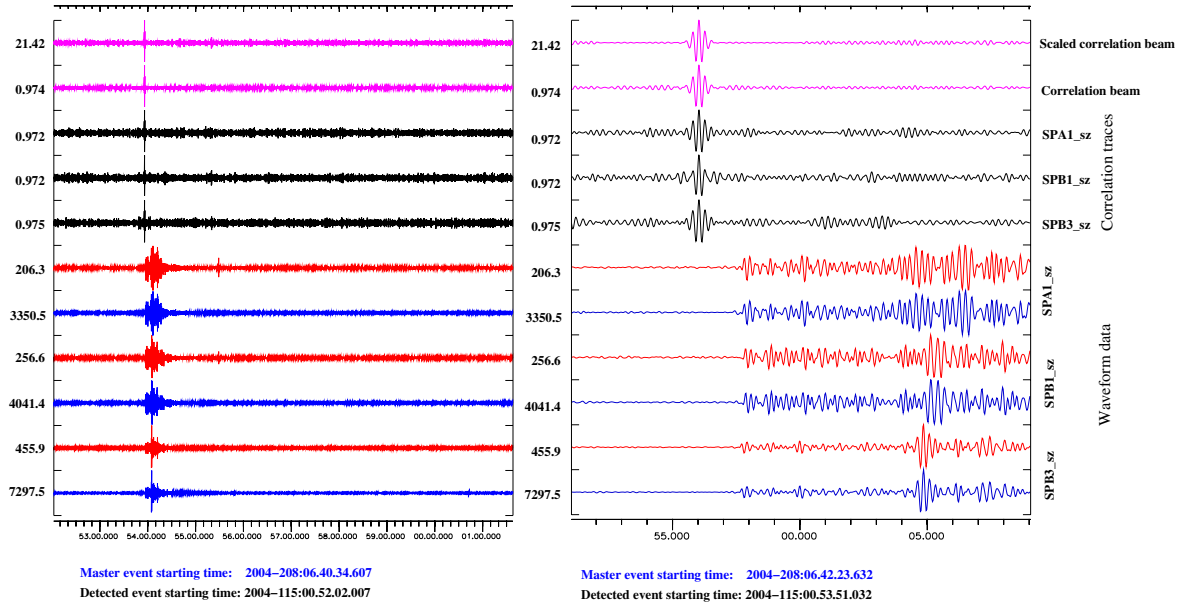

Fig. 6.1.4. The detection by waveform correlation over the Spitsbergen array of an event assumed to originate from the Barentsburg mine. Each of the red traces shows incoming waveform data in a window surrounding the cross-correlation peak and the blue traces indicate data from the master event, aligned according to the maximum correlation coefficient. The black traces indicate the correlation coefficient channels for the indicated traces between the subsequent 20 seconds of the incoming data and the extracted segment from the master event. The lowermost magenta trace, the correlation beam, C(t), is the average of all 9 single channel correlation traces over the SPITS array. For each time-point, t, we define a region of time, I_t, which is the union of two time windows: one prior to and one following t. This typically covers a few seconds of data but avoiding the immediate vicinity of time t. We calculate a scaling factor, R(t), which is the RMS value of C(t') for all t' in I_t. The scaled correlation beam, C'(t), is given by C'(t) = C(t)/R(t), and is displayed in the top trace. The right hand panel is simply a zoomed-in version of the left hand panel. All waveforms are bandpass filtered between 3.0 and 6.0 Hz. Note the alignment of the peaks of the single-channel cross-correlation traces.

In the example displayed in Figure 6.1.4, the cross-correlation coefficient exceeds 0.97 for all channels of the SPITS array; this indicates a remarkable likeness over the full length of the wavetrain, despite the fact that the amplitude of the master event is over an order of magnitude larger than that of the detected event. Note that the likeness between the different events on each channel is far greater than the likeness between the signals from each event on different channels. This indicates at the very least that the source locations of the two events are likely to be separated by a far shorter distance than the interstation distance on the Spitsbergen array.

Figure 6.1.5 illustrates another correlation detection. In this case, no signal is visible in the incoming data and any signal present clearly lies well below the noise level. However, the evidence for the presence of a signal is quite compelling; the value of the correlation beam significantly exceeds the standard deviation of the surrounding values and a close inspection of the waveforms indicate many features in common with the template waveform. Fortunately, this circumstantial evidence is compounded in this case by a clear signal recorded at the BRBB 3-component seismic station (operated by the Kola Regional Seismological Center) in close proximity of the mine.

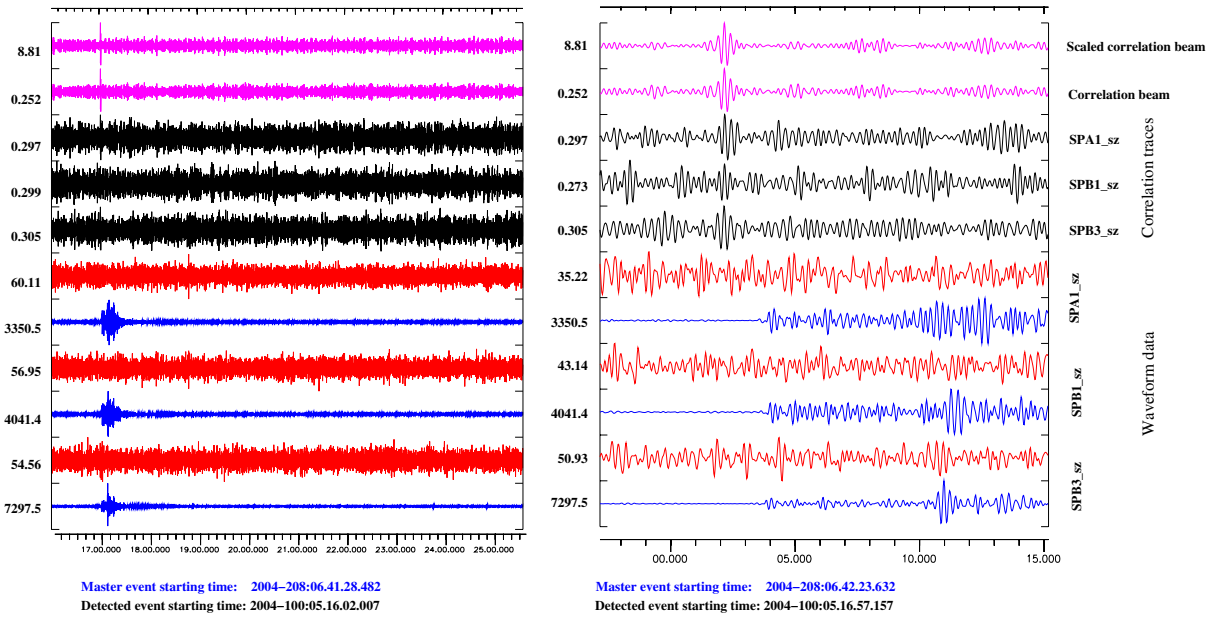

Fig. 6.1.5. A correlation detection presumed to correspond to a weak event at the Barentsburg mine. All traces are analogous to those described in Figure 6.1.5. The signal was not detectable at the SPITS array by a power detector in any frequency band. With the traces aligned according to the correlation coefficient, it is possible to observe a certain correspondence between the extreme values of the data and template waveforms on each of the channels shown. Independent evidence of the presence of an event at the mine was provided by a signal recorded by the BRBB 3-component station located close to the mine. Note that the detection is only possible by considering the full-array correlation beam; the single-channel cross-correlation traces do not even necessarily reach a global maximum at the time indicated by the correlation beam. Note also that the single-channel correlation traces are aligned in the immediate vicinity of the beam maximum.

6.1.3 The automatic screening of false alarms

The correlation detector based upon this template waveform was run on all Spitsbergen data from January 1st, 2004, until August 10th, 2004, the day on which SPITS was temporarily taken out of service for the installation of new instrumentation. A total of 7292 detections as displayed in Figures 6.1.4 and 6.1.5 were made during this period. These included the detections of many events with almost identical waveforms to those from the master event; for 4 of the detections, the array correlation coefficient exceeded 0.99, for 70 detections, the coefficient exceeded 0.90, and, for 158 detections, the coefficient exceeded 0.75. For matches with such a high degree of semblance, it is almost certain that the detection does indeed correspond to an event from the Barentsburg coal mine. However, to only accept detections in which the array correlation coefficient exceeds 0.75 would lead to the exclusion of many events such as that displayed in Figure 6.1.5, whereby the correlation coefficient is only approximately 0.25 due to the exceptionally low signal to noise ratio.

How low can we set our acceptance threshold such that we only include events which are extremely likely to come from the Barentsburg mine? The lower the permitted cross-correlation coefficient is, the more likely it is that our detection pool will include false alarms, which is to say correlation detections which result from sources unrelated to the Barentsburg mine.

An example of such a detection is displayed in Figure 6.1.6; a short high-amplitude Rg phase from an entirely different direction correlates with a short section of the master event coda sufficiently well that a detectable maximum is obtained on the array correlation beam. Not only does the detection exceed our pre-specified threshold, but the correlation coefficient is actually higher than that observed for the detection in Figure 6.1.5, which is assumed to be an event of interest. Given that, from eight months of data, we have obtained over 7000 correlation detections covering the full spectrum from “almost perfect correlation” to “marginal”, we need some form of automatic process to separate such spurious detections from those which are likely to be from the site of interest. An inspection of Figure 6.1.6 suggests a number of possible approaches. One possibility is to calculate correlation coefficients over short sections of the relevant waveforms and to compare with the full waveform correlation coefficient; this method would probably identify the example in Figure 6.1.6 as a spurious detection given that the relatively high correlation coefficient is the result of waveform semblance over a relatively short time window.

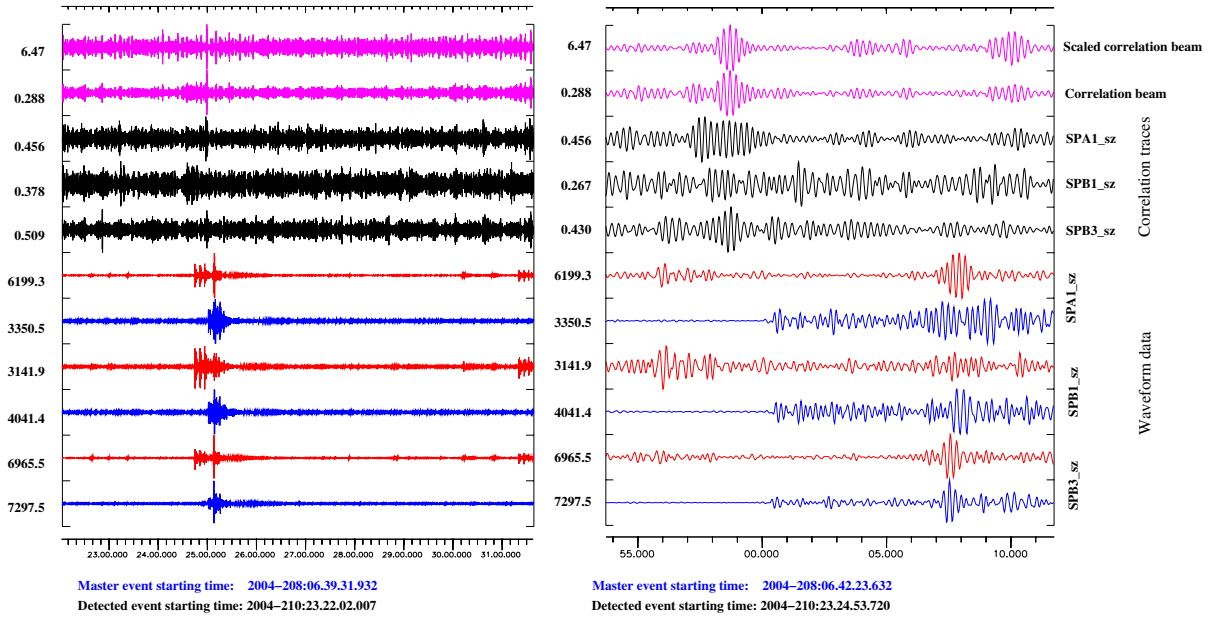

Fig. 6.1.6. A correlation detection which clearly does not correspond to an event from Barentsburg. A signal with a short time-bandwidth product correlates to such an extent with the Sg arrival of the Barentsburg template waveform that the array correlation beam results in a local maximum which triggers a detection. From plots such as these it is quite readily observed that the waveform responsible for this detection is not from our chosen site of interest. Such instances should ideally be screened out automatically. Note the poor alignment of the single channel cross-correlation traces and the fact that the value on the correlation beam is significantly less than the local maxima. on the single channel traces.

However, the most striking difference between the spurious detection in Figure 6.1.6 and the detections in Figures 6.1.4 and 6.1.5 is the alignment of the single-channel correlation coefficient traces. In the first two examples, the maximum of the correlation beam corresponds almost perfectly to local maxima of the single-channel correlation traces whereas, for the example in Figure 6.1.6, there is demonstrable destructive interference of the single-channel traces. Given that each of the single-channel correlation coefficient traces is a time series associated with a geographical site, broadband f-k analysis can be used to indicate any systematic shift in these traces in a very short time-window surrounding the time of maximum correlation on the array beam. If f-k analysis indicates that a maximum on the beam is obtained by a non-zero delay beamforming of the single traces, then it is almost guaranteed that the phase arrivals responsible for the high correlation do not come from the same direction and that, therefore, the correlation detection is spurious. Figure 6.1.7 demonstrates the results from f-k analysis from each of the examples shown in Figures 6.1.4 through to 6.1.6. The spurious detection is associated with a clearly non-zero slowness value.

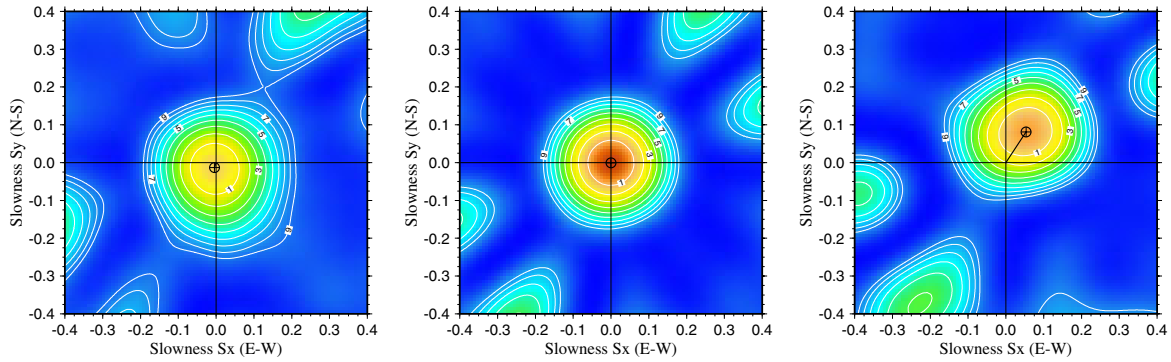

Fig. 6.1.7. Results from broadband f-k analysis on the single-channel waveform correlation traces for times 2004-100:05.17.03.210 (left: see Figure 6.1.5), 2004-157:00.53.57.089 (centre: see Figure 6.1.4), and 2004-210:23.24.59.769 (right: see Figure 6.1.6). In each case, the f-k analysis is performed in a time-window of length 1.5 seconds, centered on the given time. The relative power values obtained from the f-k calculations were 0.68 (left), 0.96 (centre), and 0.82 (right).

Whilst a clear non-zero slowness estimate from the correlation trace f-k analysis (as is shown in the right hand panel of Figure 6.1.7) essentially guarantees a false alarm, a near-zero slowness does not necessarily guarantee a true event. If the f-k power is high (as is shown in the centre panel of Figure 6.1.7), then this is a good indication that a zero time-delay stacking of the single channel correlation coefficient traces results in a beam with little energy loss and that each channel attains a maximum correlation at essentially the same time. If the f-k power is low, it may be that the best we can say is that there is insufficient evidence for a "plane wave" type optimum delay.

From our list of over 7000 correlation detections, we want to be left with only detections which are extremely likely to correspond to events from the Barentsburg mine; this means that we want to eliminate both clear false alarms and detections for which the evidence for a true correlation is not sufficiently compelling. We have already defined $C(t)$ as the correlation beam over the array; we denote the time at which $C(t)$ attains a maximum value by t_M. $C(t_M)$ is the mean value of all the single channel correlation coefficient traces obtained at a time t_M. For the correlation coefficient trace for channel i, we define the closest local maximum to time t_M as $C_i(t_M)$ (which will in general be obtained at a time t' in the immediate vicinity of t_M). If we then define $C_L(t_M)$ as the mean value of all the local maxima, $C_i(t_M)$, then the ratio $C(t_M):C_L(t_M)$ measures the amplitude of the zero-delay correlation beam relative to the amplitudes of the single-channel correlation coefficient traces. This quantity is very similar to the f-k power but is not constrained to the set of time delays permitted by plane wavefront models; a low value of $C(t_M):C_L(t_M)$ indicates that there is considerable "energy loss" in forming the beam.

For each correlation detection, we perform f-k analysis on the correlation coefficient traces and calculate the slowness and f-k power. Calculating, in addition, the quantity $C(t_M):C_L(t_M)$ we consider the detection further only if all of the following three conditions are met:

- Slowness < 0.04 s/km.
- f-k power > 0.39
- $C(t_M):C_L(t_M) > 0.58$.

These rules were arrived at simply from the manual observation of several hundred examples and examining how these quantities varied when we had a clear false alarm or a very likely Barentsburg detection. A total of 1578 detections passed the resulting test. A laborious examination of all aspects of these detections (waveforms, correlation traces, f-k analysis) indicated that there were grounds to suppose that all of these were likely to have occurred in the vicinity of the July 26th 2004 rockburst. There is an inevitable trade-off between the detection threshold imposed and the probability of obtaining false alarms. Were we to insist that the correlation coefficient, $C(t_M)$, were to exceed 0.6 for an event to be considered then we would almost certainly not have a single false alarm within our population. By lowering the detection threshold, we increase the risk of false alarms and must take appropriate steps to identify them.

6.1.4 Magnitude estimation

Once we have identified a segment of data, $v(t)$, which gives a maximum correlation with the template waveform, $v(t_0)$, we can solve for a scalar multiplier, α,which minimises the residual $|v(t) - \alpha v(t_0)|$ in the least squares sense. The validity of such an estimate will clearly diminish if the correlation coefficient is low, with a tendency for a magnitude estimate which is too low. Two temporary 3-component stations, BRBA and BRBB, situated close to the mine, provided data for selected time periods between January 1 and August 10, 2004. The best of these stations, BRBB, was operational at the times of 50 of the correlation detections and every one of these detections corresponded to a signal recorded at BRBB. The BRBA station was operational at the times of 168 correlation detections, although only 78 corresponding events were positively identified in the data. It should be noted however that the noise levels at BRBA are significantly worse than those at BRBB.

Figure 6.1.8 shows magnitude estimates for the events indicated by the cross-correlation detections obtained from both the SPITS data and from the BRBA and BRBB stations. The indications are that the magnitude estimates obtained from the cross-correlation procedure are largely consistent with the independent estimates from the on-site instruments. Poor correlation coefficients can result from both a poor signal to noise ratio and waveform dissimilarity due to differences in the source location. It is unfortunate that so much data from the on-site stations is missing.

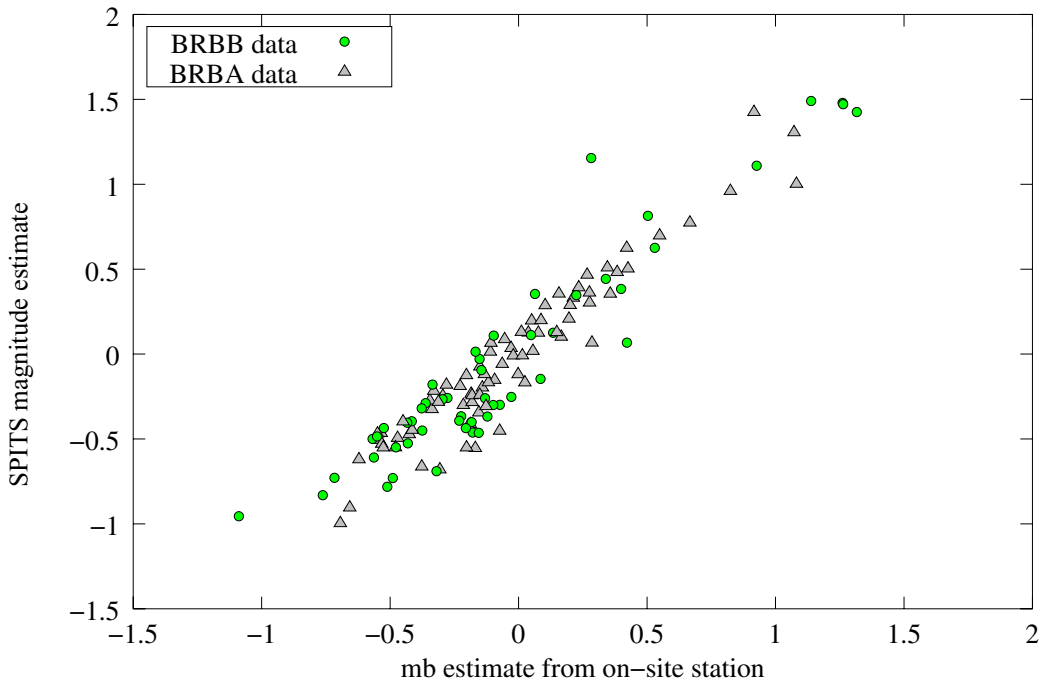

Fig. 6.1.8. Magnitude estimates of events at the Barentsburg mine from the scaling factor obtained from SPITS correlation detections and from STA values obtained from data at the on-site stations BRBA and BRBB. The master event (which was recorded by neither BRBA or BRBB) was fixed to m_b = 2.0 for the purpose of scaling.

6.1.5 A comparison of matched signal detection and detection by conventional array processing

Given a correlation detection for a presumed Barentsburg event, we know exactly when we ought to expect the appropriate P- and S- arrivals at the SPITS array. We can therefore search the detection list for SPITS and examine how many of the correlation detections correspond to events which were detected with appropriate phase propagation parameters. If we obtain a correlation detection at a time t_C, then we search for a Pg detection in the time interval [t_C - 1.2, t_C + 1.2] and an Sg detection in the interval [t_C + 5.0, t_C + 7.2]. A detection is accepted as a Barentsburg Pg phase if the apparent velocity falls within the range [6.0, 8.5] and the azimuth falls in the range [230.0, 260.0]. Similarly, a phase detection is accepted as a Barentsburg Sg if the apparent velocity falls within the range [3.0, 4.6] and the azimuth falls in the range [230.0, 260.0]. These intervals are quite large as we anticipate a certain variation in the arrival time estimates and variable frequency band slowness estimates. A site-specific reprocessing using fixed frequency band f-k analysis and autoregressive onset time estimation would almost certainly allow us to impose greater restrictions on these parameters; however, since our aim is to see how many of these events were detected by the standard processing, such an exercise is not required.

Figure 6.1.9 displays the frequency of correlation detections together with magnitude estimates from the cross-correlation calculations and a colour code to indicate whether or not a signal detection was made using the standard processing at SPITS. Altogether 1578 events were detected by the correlation method, whereas a total of 304 events were detected through con-

ventional array processing (148 with both P and S phases at SPITS, 63 with a P-phase only and 93 with an S-phase only). In the upper plot, a magnitude of -1 was chosen as a cut-off point given that no evidence exists from the on-site stations for events weaker than this. Although it is not yet clear how reliable such simple scaling magnitude estimates are as the SNR decreases, Figure 6.1.9 suggests that the detection threshold for such events has been lowered by between 0.5 and 1.0 magnitude units. An independent confirmation of this can be obtained by simply comparing the number of detections by each method, using a procedure similar to the one described by Ringdal (1974). Let us denote by C and m_c the number of events detected by the correlation procedure and the corresponding 50% detection thresholds, respectively, and let P and m_p denote similar values for conventional array processing. We then find the following approximate relationship:

$$m_p - m_c = -\frac{1}{b}\log\ (\frac{P}{C})$$

where the logarithm is to base 10 and b is the slope of the commonly used magnitude-frequency relationship for earthquakes. Setting b=1.0 and using the values above (P=304, C=1578), we obtain m_p - m_c = 0.7 magnitude units as an approximate estimate of the improvement in detectability.

It is clear that a more reliable estimate of both the absolute and relative detectability levels could be obtained if a sensitive in-mine network were available. A reference set of events detected and confirmed by such a network, as well as corresponding magnitude estimates, could then be used as a basis for a direct estimation of the detection thresholds. Clearly, this in-mine network would need to be more sensitive than the correlation procedure in order to enable such estimation to be made reliably.

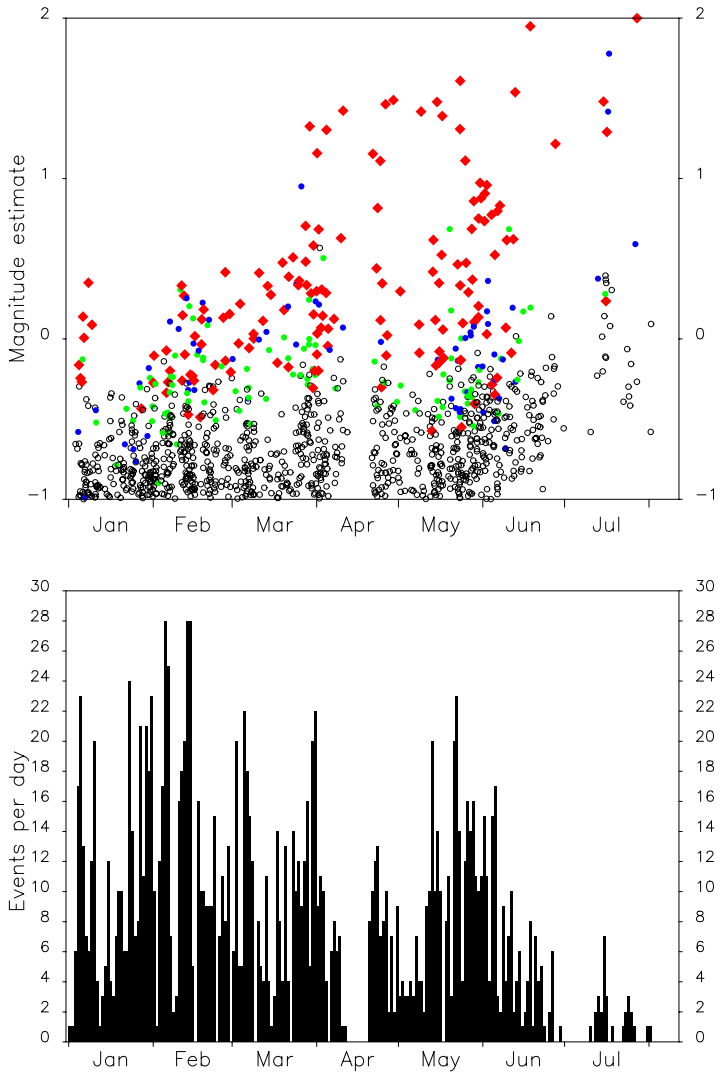

Fig. 6.1.9. The lower panel displays a histogram showing the distribution in time of the 1578 cross-correlation detections which passed the tests described in Section 6.1.3 between January 1 and August 10, 2004. The frequency with which these detections occurred is known to correspond well with industrial activity in the mine. In the upper panel, the magnitude estimate obtained from the cross-correlation calculation is displayed as a function of time. Each point is displayed as a red symbol if both a P and S detection were made at SPITS within the appropriate time windows and with appropriate propagation parameters. If only a P, but no S, phase was detected then the point is displayed as a blue symbol and a green symbol similarly indicates that an appropriate S-phase with no corresponding P-phase was detected. Black symbols indicate that either no detection was made at SPITS in the appropriate time window, or that the slowness estimates which correspond to these detections were not consistent with an event from Barentsburg.

6.1.6 Conclusions

Using waveform correlation on data from the SPITS array, with the signal from the July 26, 2004, rockburst at the Barentsburg coal mine as a template or master waveform, we have identified over 1500 instances between January 1 and August 10, 2004, for which there is evidence for the occurrence of an event located very close to the site of this incident. As the objective was to obtain a comprehensive event list, the detection thresholds were purposefully set low. The initial detection list comprised over 7000 candidate events, and many of these were clearly spurious. This made it necessary to devise a system for the automatic screening of false alarms.

False alarms generally occurred because of coincidental similarity between short sections of the template waveform and arriving phases from other sources. This problem was not encountered by Gibbons and Ringdal (2004) who ran an equivalent detection process for over two years of array data, detecting every known event from the site studied and without obtaining a single detection which did not correspond to a known event. The events sought by Gibbons and Ringdal (2004) were cavity-decoupled chemical explosions which had extremely characteristic high-frequency waveforms. The master signal and incoming data in that study were filtered in the 14 - 18 Hz frequency band as this band gave an optimal SNR. However, at such high frequencies, there is very little coherency between adjacent receivers, even for a regional array such as NORES. This, coupled with the longer length of the master signal, meant that the likelihood of coincidental correlation with unrelated signals was far smaller. The current study used a necessarily shorter time-window of data in a far lower frequency band over which the coherence (over an array with fewer stations) was far greater. Although the use of small aperture arrays is necessary for the detection of low-magnitude events using standard array processing, waveform similarity between stations appears to be a distinct disadvantage when running a matched signal detector; a more robust detector is likely when using a large aperture seismic array or a network, ideally with good azimuth coverage. We plan to carry out a systematic study of the false alarm rate as a function of network (or array) configurations, filter frequency bands and time window lengths selected for the correlation process.

The instances of correlation due to unrelated signals were readily filtered out by applying f-k analysis to the resulting waveform correlation traces and applying a set of predetermined rules. Many borderline cases with a very low SNR were also removed in this process; these may have corresponded to Barentsburg events but there was insufficient evidence at the SPITS array to support this. This procedure reduced the list of detections from over 7000 to 1578. Of these, a large number correspond to detections made by standard processing at the SPITS array and many others covering a wide range of magnitudes were also registered by two on-site three component instruments close to the Barentsburg mine. The distribution in time of detections appears to correspond well with activity at the mine during the period investigated.

References

Geller, R. J. and Mueller, C. S. (1980). Four Similar Earthquakes in Central California. *Geophys. Res. Lett.*, **7**, 821-824.

Gibbons, S. J. and Ringdal, F. (2004). A waveform correlation procedure for detecting decoupled chemical explosions, Semiannual Technical Summary, 1 January - 30 June 2004, NORSAR Sci. Rep. 2-2004, Norway. pp 41-50.

Kremenetskaya, E., Baranov, S., Filatov, Y., Asming, V. E. and Ringdal, F. (2001). Study of seismic activity near the Barentsburg mine (Spitsbergen), Semiannual Technical Summary, 1 October 2000 - 30 June 2001, NORSAR Sci. Rep. 1-2001, Norway. pp 114-121.

Kværna, T., Schweitzer, J., Ringdal, F., Asming, V. and Kremenetskaya, E. (2003): Seismic events associated with the Barentsburg mining accident on 7 June 2003, Semiannual Technical Summary, 1 January - 30 June 2003, NORSAR Sci. Rep. 2-2003, Norway. pp 77-86.

Nakahara, H. (2004). Correlation distance of waveforms for closely located events - I. Implications of the heterogeneous structure around the source region of the 1995 Hyogo-Ken Nanbu, Japan, earthquake (M_W = 6.9), Geophys. J. Int., **157**, 1255-1268.

Ringdal, F., Kværna, T., Kremenetskaya, E. O., Asming, V., Mykkeltveit, S., Gibbons, S. J. and Schweitzer, J. (2003). Research in Regional Seismic Monitoring. Proceedings of the 25th Seismic Research Review - Nuclear Explosion Monitoring: Building the Knowledge Base. September 23-25, 2003, Tucson Arizona. pp 291-300.

Ringdal, F., (1974). Estimation of seismic detection thresholds, Report No. ALEX(01)-TR-74-02, Texas Instruments Inc., Dallas, Texas.

Acknowledgements

We would like to thank Vladimir Asming at the Kola Regional Seismological Center, Apatity, Russia for analysis of 3-component data from the stations close to the Barentsburg mine.

S. J. Gibbons
F. Ringdal